Fractal Antennas in Telecommunication Technologies

Z.Zh. Zhanabaev, M.K. Ibraimov
Department of Physics and Technology, IETP,
Al-Farabi Kazakh National University
Almaty, Kazakhstan
e-mail: beibitkaribaev7@gmail.com

A.K. Imanbayeva, B.A. Karibayev, T.A. Namazbayev
Department of Physics and Technology, NNLOT,
Al-Farabi Kazakh National University
Almaty, Kazakhstan
e-mail: akmaral@physics.kz

***Abstract*—The paper provides the results of an experimental and theoretical study of a fractal dipole antenna based on an anisotropic fractal. It shows that the anisotropic fractal antenna has the maximum signal-to-noise ratio in comparison with other known fractal antennas.**

Keywords—fractal; antenna; capture power; signal-to-noise ratio

I. INTRODUCTION

Antennas are an important element of radio transmitting and receiving devices. The modern means of radio communication contains various wireless technologies, operating simultaneously in different frequency ranges, and the development of new ranges in communication, broadcasting, navigation, radiolocation, etc. is also increasing. Currently, the main research in the field of antenna-feeder devices is aimed at developing multi-band antennas and reducing the size due to the trend of mobile devices in minimum size [1,2]. Particular attention is being paid to fractal antennas.

The concept of fractal, which was introduced by Mandelbrot [3], found wide application in various fields of science and technology, including radio engineering. The structure of the fractal is self-similar at different scales. Due to this feature, antennas based on this geometry have the multi-band property. In recent years, a number of fractal antennas in various designs (wire, strip, antenna array, etc.) have been studied and developed for the generation of mobile communications, wi-fi, navigation, radar and for small-size satellites [4-7]. Therefore, an important question arises, which fractal antenna has effectivency in terms of electrodynamic properties, unlike others, under the same measurement conditions and characteristic parameters.

The theory of non-integer dimensional and multi-fractional spaces is used to describe fractals. This theory of fractional and non-integer dimensional spaces allows us to take into account the anisotropy of the fractal media in the framework of continuum models. We apply this theory as a tool for describing anisotropic fractal geometry. The purpose of this paper is to study the features of a wire dipole fractal antenna based on an anisotropic geometric fractal (AF) [8], and to compare the capture power and signal-to-noise ratio (SNR) of a given antenna with others, which have extreme differences in the deformation of the prefractals: the "isotropic" Minkowski fractal (IF) and the Koch triangular fractal (KF).

II. ANISOTROPIC FRACTAL AND ANALYTICAL DESCRIPTION OF ITS CHARACTERISTICS

In an anisotropic geometric fractal with an increase in the prefractal number (hierarchical level), the ∏-shaped parts are formed only in one direction, with the side links not deformed (Fig.1a). The prefractal dimension D=ln5/ln3=1.4649 is realized only in one direction.

We use the Heaviside function $\theta(x)$ to construct an anisotropic fractal. By entering the level (A) and the quantity (k) of the Heaviside function, we can analytically describe any of the prefractals by the following formula:

$$y = \sum_{i=1}^{n}\left(\frac{A}{3^{n-1}}\right)\sum_{k=1}^{3^n}\left((-1)^{k+1}\theta\left(x-\frac{k}{3^n}\right)\right), k \neq 3s, \quad (1)$$

$$\theta(x) = \begin{cases} 1, & x > 0 \\ 0, & x < 0 \end{cases}$$

where n is the number of iterations, A is the amplitude of function $y(x)$. Figure 1.b shows the anisotropic fractal (AF) for $n = 3$ according to (1). Elements of other fractals are deformed in different changing directions, which make it difficult to choose the formula of the construction algorithm. Therefore, a geometrically recursive algorithm is usually used.

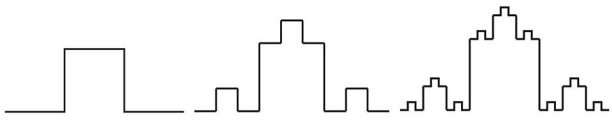

a)

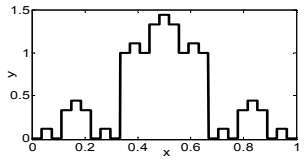

b)

Fig. 1. Structure of an anisotropic fractal. Prefractals with iteration numbers n = 1,2,3 (a), a fractal curve constructed according to formula (1) (b).

A. Electrodynamic characteristics

For fractal antennas, the usual theory of the electromagnetic field, based on the system of Maxwell's equations, is inapplicable, since fractal geometry is jumplike. We will use the condition that the maximum radiation of the antenna is achieved when the wavelength is equal to the fractal length of the antenna.

The electric field strength $E(r,t)$ of the electromagnetic wave can be represented in the form:

$$\boldsymbol{E}=\boldsymbol{E_0}exp(-i(\omega t-\boldsymbol{kr})), \quad (2)$$

where ω is the cyclic frequency, $\boldsymbol{k}$ is the wave vector, $\boldsymbol{r}$ is the radius vector of the observation point E. If we consider the wave propagation only in the x direction, then:

$$\boldsymbol{kr}=kx\cos\theta, \quad (3)$$

where θ is the angle between the directions of x and k. From (2) и (3) follows the condition for realizing the maximum $E=E_0$ with respect to time and space:

$$\omega t - kx\cos\theta = 0,\ \omega = \boldsymbol{kv} = \cos\theta, \quad (4)$$

where $k=2\pi/\lambda$ is the wave number, λ is the wavelength, $\omega=2\pi f$ is cyclic frequency, $v=x/t$ is the wave propagation velocity. From (4) we have:

$$\cos\theta = \omega t/kx, \text{ from here } \theta = 2\pi m \pm arccos\,(wt/kx), \quad (5)$$

where m is any integer, $arccos(\omega t/kx)$ is the value enclosed between 0 и π. The length of the antenna is chosen equal to the wavelength of the received radiation ($L=\lambda$). For a fractal structure, L is defined as a fractal measure [9]:

$$L=L_0\delta^{-(D-d)n} = L_0\delta^{-n\gamma},\ \gamma=D-d \quad (6)$$

where L_0 is the non-fractal (regular) antenna length, δ is the dimensionless measurement scale, D, d are the fractal and topological antenna dimensions, and n is the prefractal number (hierarchical generation). Then (5) can be written in the form:

$$\theta = 2\pi m \pm arccos\,((L_0/v)\,\delta^{-n\gamma} f). \quad (7)$$

We use the equation of electron motion with a charge e, mass m_e under the action of the force $-eE$ in the x coordinate:

$$m_e(d^2x/dt^2) = -eE. \quad (8)$$

Taking into account (3) and (4) from the (8) we define the square of the electric field strength, to which the energy of electromagnetic radiation is proportional:

$$E_x^2 = (m_e/e)^2x^2(kv)^4\cos^4\theta. \quad (9)$$

We write the (9) in the dimensionless form:

$$(E_x/E_{0x})^2 = (kv/\omega_0)^4\cos^4\theta \quad (10)$$

where $E_{ox}^2 = \omega_0^4(m_e/e)^2x^2$, ω_0 can be taken as the electron plasma frequency. Assuming the constants, ω_0 and taking into account $k=2\pi/\lambda=2\pi/L_0\delta^{-n\gamma}$ we obtain the law of energy distribution over the antenna radiation angle θ with the prefractal order n, with the scaling exponent $\gamma=D-d$ at a distance x from the antenna:

$$(E_x/E_{0x})^2 = \delta^{4n\gamma}\cos^4\theta\,. \quad (11)$$

B. Signal-to-noise ratio

Radio engineering devices require a high-precision estimation of the signal-to-noise ratio (SNR) to achieve the quality and efficiency of the transceiving telecommunication nodes. The signal-to-noise ratio is a dimensionless quantity, which is defined as:

$$SNR(dB)=10\,log_{10}(P_{signal}/P_{noise}), \quad (12)$$

where P_{signal} is useful signal power, P_{noise} is noise power.

III. Experimental Setup and Prototypes of Antennas

Fig. 2 shows the prototypes of the antennas under consideration in the prefractal with n=2. KF (with fractal dimension is D=1.26, δ=1/3) is formed by dividing into three equal parts of a single segment and replacing the middle interval by an equilateral triangle without this segment (Fig.2b). The IF is shown in Fig.2c. The generator of this fractal (D=1.5, δ=1/4) consists of eight links with a length of 1/4. All links are deformed in all directions with the growth of the prefractal number. The regular length of the selected antenna samples is L_0 = 7 cm, and the gap between radiators is g = 0.5 cm. Table 1 shows the fractal lengths L of antennas, which are defined by (6).

TABLE I. Fractal Lengths of Antennas

Iteration Number	Fractal Lengths *L* of Antennas, cm		
	AF	***KF***	***IF***
1	23.33	18.66	28.05
2	32.66	24.88	56.05
3	42.00	33.18	112.05

Fig. 3 shows the experimental setup for measuring the captured power of fractal antennas in the range 0.1 - 3.0 GHz and its block diagram. The signal generator NI PXI-5652 (where -5 dBm is installed) and the Agilent N9340B spectrum analyzer were used to generate and receive the signal, respectively (Fig. 3a). The antenna prototypes were connected to the measuring devices by coaxial cables and SMA connectors. The experimental conditions were the same for all types of antennas. The measurements were carried out in two versions (Fig. 3b): the first – the plane of the fractal antenna XZ was perpendicular to the Y axis, along which the emitting horn is located at a distance of 2 m, the second - the plane of

the antenna YZ is parallel to the Y axis. Finally, the amplitudes of the power in the frequency band were displayed in the graphical interface (in Labview) and the digital data was recorded. According to the received data, the average values of the captured capacities were calculated. The noise characteristics were measured to determine the SNR values of each antenna. To do this, each sample was connected to a spectrum analyzer, which recorded all background noise in the same range of 0.1–0.3 GHz. Their average values $<P_{noise}>$ were also determined.

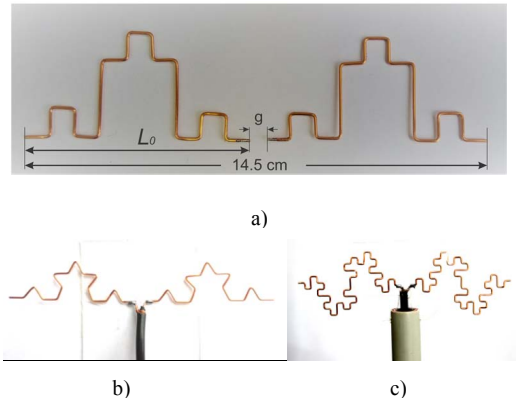

Fig. 2. Antenna prototypes for $n = 2$ fractals.

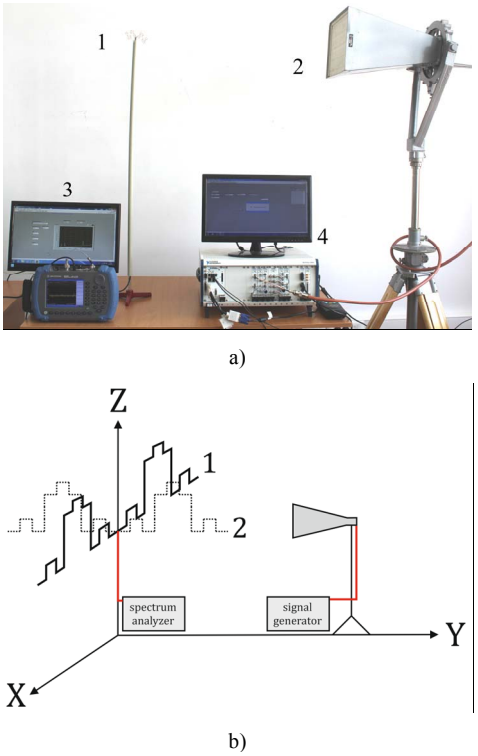

Fig. 3. The hardware-software system of the experimental setup. 1-fractal antenna, 2 - horn antenna, 3 - spectrum analyzer with PC, 4 - RF signal generator with control PC (a), antenna plane orientations 1 and 2 (b).

IV. Results and Discussion

Table 2 shows the SNR values for antennas for each prefractal number obtained by calculation using (11) and (12). The mean values of $(E_x/E_{0x})^2$ were determined in the range 0.1-3.0 GHz, where E_x^2 is proportional value to the capture power of antenna. The measured values E_{0x}^2 of the antennas by a physical experiment were used as noise. The table 2 shows that the AF antenna has relatively large SNR values in $n = 2,3$ than the KF and IF antennas.

TABLE II. Theoretical SNR of Fractal Antennas

Iteration Number	SNR of Antennas, dB		
	AF	*KF*	*IF*
1	16,81	20,00	16,03
2	17,00	15,80	6,62
3	17,08	10,83	2,92

Fig. 4 and 5 shows the measurement results the power spectrum of received radiation of antenna (n=2) in different cases of antenna location shown in the Fig. 3b. All antennas receive signals with a low level (below -60 dBm), the levels of the received signals increase from the frequency of 0.55 GHz (Fig. 4). This is observed in the first measurement case (the plane of the antenna is perpendicular to the direction of propagation of the received wave) in the range 0.1–0.5 GHz. Further, sharp drops and rises in different frequencies are observed for each antenna. The average value of the received power of the AF antenna (- 37.79 dBm) is higher than the rest antennas (average powers of KF and IF are -38.64 dBm and -40.69 dBm, respectively). The same picture is observed in the case where the plane of the antenna and the direction of the maximum radiation of the horn antenna are parallel. All antennas take a minimum of power to the frequency of 0.5 GHz, amplitude oscillations in frequency are observed above this frequency (Fig. 5). It is also seen that the AF antenna takes relatively large powers. Note that the theoretical value of SNR (see Table 2) for the case n=1 of AF antenna is lower, than KF antenna due to the establishment of scale invariance in n = 2.

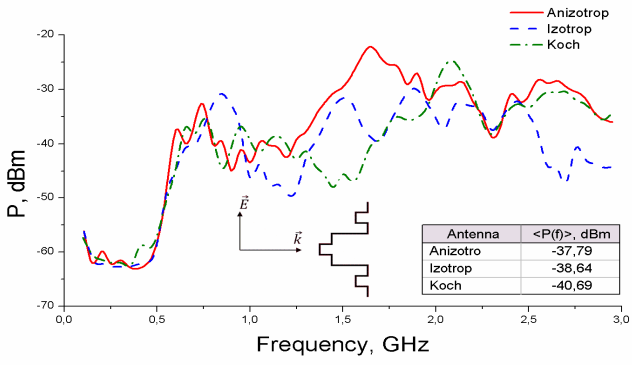

Fig. 4. The power spectrum of the fractal antennas at $n = 2$ for the first measurement case.

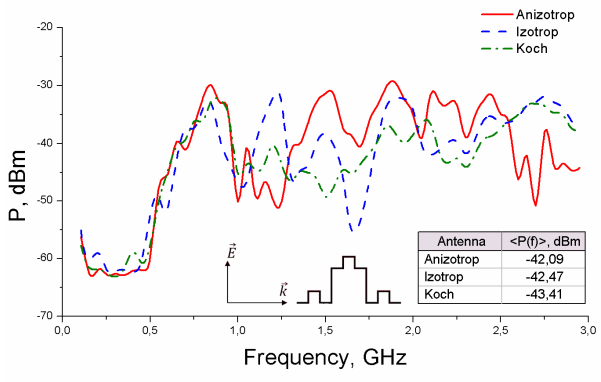

Fig. 5. The power spectrum of the fractal antennas at $n = 2$ for the second measurement case.

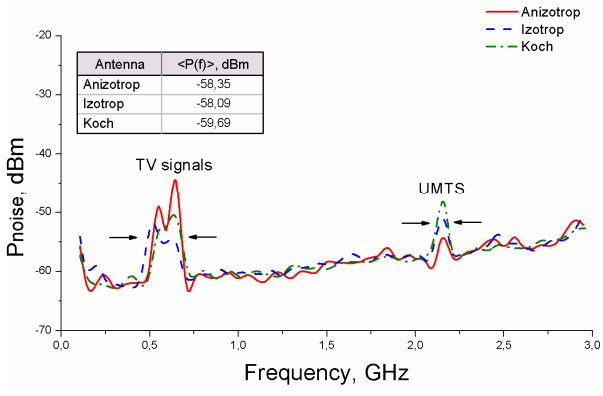

Fig. 6. Measured background noise of fractal antennas at $n = 2$.

TABLE III. EXPERIMENTAL SNR OF FRACTAL ANTENNAS

Iteration Number	SNR of Antennas, dB		
	AF	***KF***	***IF***
1	19,75	17,00	17,50
2	20,55	19,00	19,50
3	20,50	17,00	20,00

The power of radiation received by fractal antenna depends on the capture area determined by the length of antenna L (wavelength λ). AF antenna with a smaller fractal length than the IF antenna receives more power due to the one-way directivity of the anisotropic antenna. Also, AF antenna with a relatively small physical cross-sectional area has a capture area that is significantly larger than its physical size and has large gain.

Fig. 6 demonstrates the background noise of antennas in frequency. It should be noted that the present TV and UMTS signals, which have a significantly higher level than the background noise, were not taken into account when determining the mean value of noise. SNR values of antennas have been determined by the (12), the results of which are given in Table 3. It can be seen that all the prefractals of the AF antenna have a signal-to-noise ratio exceeding the IF and KF antenna levels.

V. CONCLUSION

In this paper, we compared three types of wire dipole antennas based on geometric fractals: anisotropic, Koch and Minkowski curves. Their capture power was measured experimentally at the same regular lengths. The effectiveness of the AF antenna when receiving radio waves in a wide range (0.1-3.0 GHz) is shown, which is associated with a relatively large effective capture area. The signal-to-noise ratios of the examined antennas were determined experimentally and theoretically. It is shown that the AF antenna has a relatively high signal-to-noise level.

This property of the anisotropic fractal antenna allows them to be used in multi-band wireless communication technologies and in radar, including for passive radars [10], using a wide frequency range. The new fractal considered by us also has the simplest technological construction for the purpose of manufacturing automatically assembling antennas, miniaturization of radio modules and deployable elements of robotics.

ACKNOWLEDGMENT

This work has been supported by the Ministry of Education and Science of Kazakhstan under Grants numbers AP05132738 and BR05236494

REFERENCES

[1] H.Z. Ding, Y.C. Jiao and T.Ni, “A compact multiband printed antenna for smart-phone applications,” Microwave and Optical Technology Lett, vol. 57, pp. 2289-2294, 2015.

[2] P. Bartwal, A.K. Gautam, A.K. Singh, B.K. Kanaujia and K. Rambabu, “Design of compact multi-band meander-line antenna for global positioning system/wireless local area network/worldwide interoperability for microwave access band applications in laptops/tablets,” IET Microwaves Antennas & Propagation, vol. 10, pp. 1618-1624, 2016.

[3] B. Mandelbrot, Les Objects Fractals: Forme, Hasard et Dimension. Paris: Flammarion, 1975.

[4] M. Gupta and V. Mathur, “A new printed fractal right angled isosceles triangular monopole antenna for ultra-wideband application,” Egyptian Informatics Journal, vol. 18, pp. 39-43, 2017.

[5] Z. Yu, J. Yu, X. Ran and C. Zhu, “A novel Koch and Sierpinski combined fractal antenna for 2G/3G/4G/5G/WLAN/navigation applications,” Microwave and Optical Technology Letters, vol. 59, pp. 2147-2155, 2017.

[6] Z.Z. Zhanabaev, B.K. Karibayev, T.A. Namazbayev, A.A. Imanbayeva, A.A. Temirbayev and S.N. Ahtanov, “Fractal Antenna with Maximum Capture Power,” ACM International Conference Proceeding Series. 6th International Conference on Telecommunications and Remote Sensing Delft, Netherlands, pp. 17-20, 2017, DOI: 10.1145/3152808.3152811.

[7] J. Simon, J.L. Alvarez-Flores, J. Villanueva-Maldonado, V.H. Castillo-Topete, L. Soriano-Equigua and J. Flores-Troncoso, “A microstrip second-iteration square Koch dipole antenna for TT&C downlink applications in small satellites,” International Journal of Antennas and Propagation. DOI: 10.1155/2017/4825179.

[8] Z. Zhanabaev, “Fractal model of turbulence in the jet,” Proceedings of the SB Acad.of Sci.USSR, vol. 4, pp. 57-60, 1988.

[9] J.Feder, Fractals. Plenum Press, New York, 1988.

[10] A. Zaimbashi, “Target Detection in Analogue Terrestrial TV-based Passive Radar Sensor: Joint Delay-Doppler Estimation,” IEEE Sensors Journal, vol. 17, pp. 5569-5580, 2017.